CHAPTER 9

SURFACE RADIATIVE EXCHANGE IN THE PRESENCE OF CONDUCTION AND CONVECTION

9.1 INTRODUCTION

In the previous few chapters we have considered only the analysis of radiative exchange in enclosures with specified wall temperatures or fluxes, i.e., we have neglected interaction with other modes of heat transfer. In practical systems, of course, it is nearly always the case that radiation from a boundary is affected by conduction into the solid and/or by convection from the surface. Then, two or three modes of heat transfer must be accounted for simultaneously. The interaction may be quite simple, or it may be rather involved. For example, heat loss from an isothermal surface of known temperature, adjacent to a radiatively nonparticipating medium, may occur by convection as well as radiation; however, convective and radiative heat fluxes are independent of one another, can be calculated independently, and may simply be added. If boundary conditions are more complex (i.e., surface temperatures are not specified), then radiation enters the remaining conduction/convection problem as a nonlinear boundary condition.

In a number of important applications, a conduction analysis needs to be performed on an opaque medium, which loses (or gains) heat from its surfaces by radiation (and, possibly, convection). In such cases radiation enters the conduction problem as a nonlinear boundary condition; however, the radiative flux in this boundary condition may depend on the radiative exchange in the surrounding enclosure. In other applications, conduction and/or convection in a transparent gas or liquid needs to be evaluated, bounded by opaque, radiating walls. Again, radiation enters only as a boundary condition, with the transparent medium itself occupying the enclosure governing the radiative transfer. In both types of applications radiation and conduction–convection are interdependent, i.e., a change in radiative heat flux disturbs the overall energy balance at the surface, causing a change in temperature as well as conductive–convective fluxes, and vice versa.

Many important applications of interactions between surface radiation and other modes of heat transfer have been reported in the literature. We will limit ourselves here to the discussion

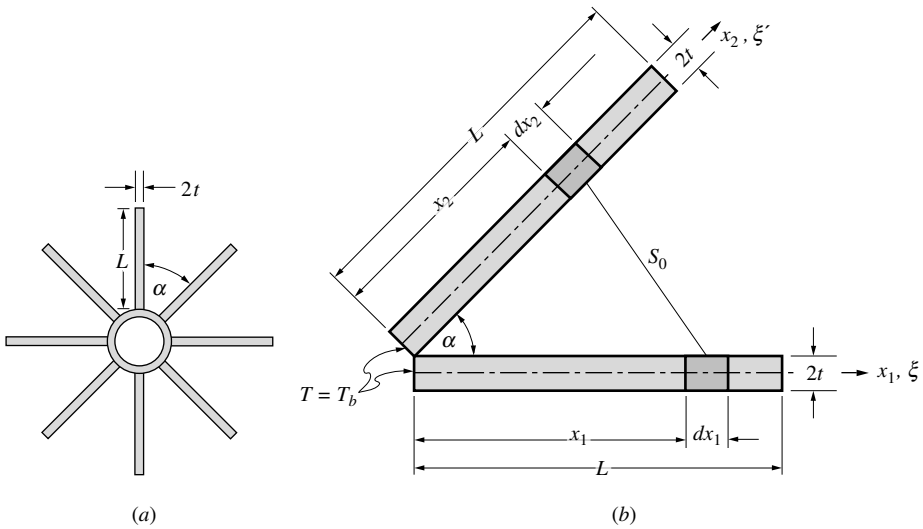

FIGURE 9-1
Schematic of a space radiator tube with longitudinal fins.

of a few very basic cases (*i*) to show the basic trends of how the different modes of heat transfer interact with one another, and (*ii*) to outline some of the numerical schemes that have been used to solve such problems. At the end of each section a short description of more advanced problems is given, as well as a list of references.

9.2 CONDUCTION AND SURFACE RADIATION—FINS

The vast majority of combined conduction–surface radiation applications involve heat transfer through vacuum, e.g., heat loss from space vehicles or vacuum insulations. As a single example we will discuss here the performance of a simple rectangular-fin radiator used to reject heat from a spacecraft.

Consider a tube with a set of radial fins, as schematically shown in Fig. 9-1. In order to facilitate the analysis, we will make the following assumptions:

1. The thickness of each fin, $2t$, is much less than its length in the radial direction, L, which in turn is much less than the fin extent in the direction of the tube axis. This implies that heat conduction within the fin may be calculated by assuming that the fin temperature is a function of radial distance, x, only.

2. End losses from the fin tips (by convection and radiation) are negligible, i.e., $\partial T_i/\partial x_i\,(L) \simeq 0$.

3. The thermal conductivity of the fin material, k, is constant.

4. The base temperatures of all fins are the same, i.e., $T_1(0) = T_2(0) = T_b$, and the fin arrangement is symmetrical, i.e., $T_1(x_1) = T_2(x_2 = x_1)$, etc.

5. The surfaces are coated with an opaque, gray, diffusely emitting and reflecting material of uniform emittance ϵ.

6. There is no external irradiation falling into the fin cavities ($H_o = 0,\ T_\infty = 0$).

The first three assumptions are standard simplifications made for the analysis of thin fins (see, e.g., Holman [1]), and the other three have been made to make the radiation part of the

problem more tractable. Performing an energy balance on an infinitesimal volume element (of unit length in the axial direction) $dV = 2t\,dx$, one finds:

conduction going in at x across cross-sectional area $(2t)$
= conduction going out at $x+dx$
+ net radiative loss from top and bottom surfaces $(2\,dx)$

or

$$-2tk\left.\frac{dT}{dx}\right|_x = -2tk\left.\frac{dT}{dx}\right|_{x+dx} + 2q_R\,dx.$$

Expanding the outgoing conduction term into a truncated Taylor series,

$$\left.\frac{dT}{dx}\right|_{x+dx} = \left.\frac{dT}{dx}\right|_x + dx\left.\frac{d^2T}{dx^2}\right|_x + \cdots,$$

then leads to

$$\frac{d^2T}{dx^2} = \frac{1}{tk}\,q_R. \tag{9.1}$$

Here $q_R(x)$ is the net radiative heat flux leaving a surface element of the fin, which may be determined in terms of surface radiosity, J, from equations (5.24) and (5.25) as[1]

$$q_R(x_1) = J(x_1) - \int_{x_2=0}^{L} J(x_2)\,dF_{d1-d2}, \tag{9.2}$$

$$J(x_1) = \epsilon\sigma T^4(x_1) + (1-\epsilon)\int_{x_2=0}^{L} J(x_2)\,dF_{d1-d2}. \tag{9.3}$$

The expression for radiative heat flux may be simplified by eliminating the integral, equation (5.26),

$$q_R(x_1) = \frac{\epsilon}{1-\epsilon}\left[\sigma T_1^4(x_1) - J_1(x_1)\right]. \tag{9.4}$$

The view factor between two infinitely long strips may be found from Appendix D, Configuration 5, or from Example 4.1 as

$$F_{d1-d2} = \frac{x_1\sin^2\alpha\,x_2\,dx_2}{2S_0^3} = \frac{\sin^2\alpha\,x_1x_2\,dx_2}{2(x_1^2 - 2x_1x_2\,\cos\alpha + x_2^2)^{3/2}}. \tag{9.5}$$

Equation (9.1) requires two boundary conditions, namely,

$$T(x=0) = T_b, \quad \frac{dT}{dx}(x=L) = 0. \tag{9.6}$$

Before we attempt a numerical solution, it is a good idea to summarize the mathematical problem in terms of nondimensional variables and parameters,

$$\theta(\xi) = \frac{T(x)}{T_b}, \quad \mathscr{J}(\xi) = \frac{J(x)}{\sigma T_b^4}, \quad N_c = \frac{kt}{\sigma T_b^3 L^2}, \quad \xi = \frac{x}{L}, \tag{9.7}$$

[1]For the radiative exchange it is advantageous to attach subscripts 1 and 2 to the x-coordinates to distinguish contributions from different plates, even though $T(x)$, $J(x)$, $q_R(x)$, etc., are the same along each of the fins.

where θ and $\mathscr{J}$ are nondimensional temperature and radiosity, and N_c is usually called the *conduction-to-radiation parameter*, sometimes also known as the *Planck number*. With these definitions,

$$\frac{d^2\theta}{d\xi^2} = \frac{1}{N_c}\frac{\epsilon}{1-\epsilon}\left[\theta^4(\xi) - \mathscr{J}(\xi)\right], \tag{9.8a}$$

$$\mathscr{J}(\xi) = \epsilon\,\theta^4(\xi) + (1-\epsilon)\int_{\xi'=0}^{1} \mathscr{J}(\xi')\,K(\xi,\xi')\,d\xi', \tag{9.8b}$$

$$K(\xi,\xi') = \frac{1}{2}\sin^2\alpha\,\frac{\xi\,\xi'}{(\xi^2 - 2\xi\xi'\cos\alpha + \xi'^2)^{3/2}}, \tag{9.8c}$$

subject to

$$\theta(\xi=0) = 1, \quad \frac{d\theta}{d\xi}(\xi=1) = 0. \tag{9.8d}$$

As for convection-cooled fins, a *fin efficiency*, η_f, is defined, comparing the heat loss from the actual fin to that of an ideal fin (a black fin, which is isothermal at T_b). The total heat loss from an ideal fin ($\epsilon = 1$, $J = \sigma T_b^4$) is readily determined from equation (9.2) and Appendix D, Configuration 34, as

$$Q_{\text{ideal}} = 2L\,q_{R,\text{ideal}} = 2L\,\sigma T_b^4(1 - F_{1-2}) = 2L\,\sin\frac{\alpha}{2}\sigma T_b^4, \tag{9.9}$$

while the actual heat loss follows from Fourier's law applied to the base, or by integrating over the length of the fin, as

$$Q_{\text{actual}} = -2tk\left.\frac{dT}{dx}\right|_{x=0} = 2\int_0^L q_R(x)\,dx. \tag{9.10}$$

Thus,

$$\eta_f = \frac{Q_{\text{actual}}}{Q_{\text{ideal}}} = -\frac{N_c}{\sin\frac{\alpha}{2}}\left.\frac{d\theta}{d\xi}\right|_0 = \frac{1}{\sin\frac{\alpha}{2}}\frac{\epsilon}{1-\epsilon}\int_0^1 (\theta^4 - \mathscr{J})\,d\xi, \tag{9.11}$$

where the last expression is obtained by integrating equation (9.8*a*) along the length L of the fin.

The set of equations (9.8) is readily solved by a host of different methods, including the net radiation method [finite-differencing equation (9.8*b*) into finite-width isothermal strips, to which equation (5.34) can be applied] or any of the solution methods for Fredholm equations discussed in Section 5.6. Because of the nonlinear nature of the equations it is always advisable to employ the method of successive approximations, i.e., a temperature field is guessed, a radiosity distribution is calculated, an updated temperature field is determined by solving the differential equation (for a known right-hand side), etc.

Sample results for the efficiency, as obtained by Sparrow and coworkers [2], are shown in Fig. 9-2. The variation of the fin efficiency is similar to that for a convectively cooled fin (with the heat transfer coefficient replaced by a "radiative heat transfer coefficient," $h_R = 4\epsilon\sigma T_b^3$). Maximum efficiency is obtained for $N_c \to \infty$, i.e., when conduction dominates and the fin is essentially isothermal. For $\epsilon < 1$ the efficiency is limited to values $\eta_f < 1$ since a black configuration will always lose more heat. It is also observed that the fin efficiency (but not the actual heat lost) increases as the opening angle α decreases: For small opening angles irradiation from adjacent fins reduces the net radiative heat loss by a large fraction, but not as much as for the "ideal" fin (with irradiation from adjacent fins, which are black and at T_b).

Many other studies discussing the interaction of surface radiation and one-dimensional conduction may be found in the literature. For example, Hering [3] and Tien [4] considered the fins of Fig. 9-1 with specularly reflecting surfaces, and Sparrow and coworkers [2] investigated the influence of external irradiation. Fins connecting parallel tubes were studied by Bartas and Sellers [5], Sparrow and coworkers [6, 7], and Lieblein [8]. Single annular fins (i.e., annular

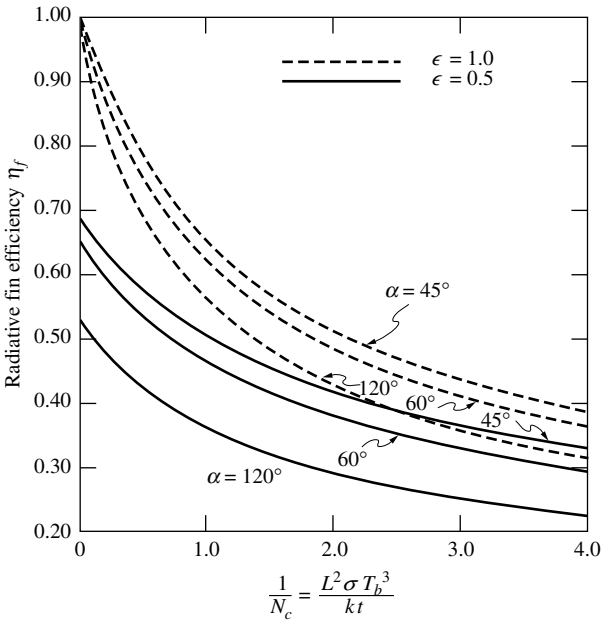

FIGURE 9-2
Radiative fin efficiency for longitudinal plate fins [2].

disks attached to the outside of tubes) were studied by Chambers and Sommers [9] (rectangular cross-section), Keller and Holdredge [10] (variable cross-section), and Mackay [11] (with external irradiation), while Sparrow and colleagues [12] investigated the interaction between adjacent fins. Various other publications have appeared dealing with different geometries, surface properties (including nongrayness effects), irradiation conditions, etc. A partial listing is given with [13–35].

More recently, some researchers have considered combined conduction–surface radiation in media with cavities, such as porous media [36, 37], packed beds of spheres [38], mirror furnaces [39], and honeycomb panels [40–42].

9.3 CONVECTION AND SURFACE RADIATION

As in the case of pure convection heat transfer, it is common to distinguish between external flow and internal flow applications. If the flowing medium is air or some other relatively inert gas, the assumption of a transparent, or radiatively nonparticipating, medium is often justified. As an example we will consider here the case of a transparent gas flowing through a cylindrical tube of diameter $D = 2R$ and length L, which is heated uniformly at a rate of q_w (per unit surface area). As schematically shown in Fig. 9-3, the fluid enters the tube at $x = 0$ with a mean, or bulk, temperature T_{m1}. Over the length of the tube the supplied heat flux q_w is dissipated from the inner surface by convection (to the fluid) and radiation (to the openings and to other parts of the tube wall), while the outer surface of the tube is insulated. The two open ends of the tube are exposed to radiation environments at temperatures T_1 and T_2, respectively. The inner surface of the tube is assumed to be gray, diffusely emitting and diffusely reflecting, with a uniform emittance ϵ. Finally, for a simplified analysis, we will assume that the convective heat transfer coefficient, h, between tube wall and fluid is constant, independent of the radiative heat transfer, and known.

With these simplifications an energy balance on a control volume $dV = \pi R^2 \times dx$ yields:

$$\text{enthalpy flux in at } x + \text{convective flux in over } dx = \text{ enthalpy flux out at } x+dx,$$

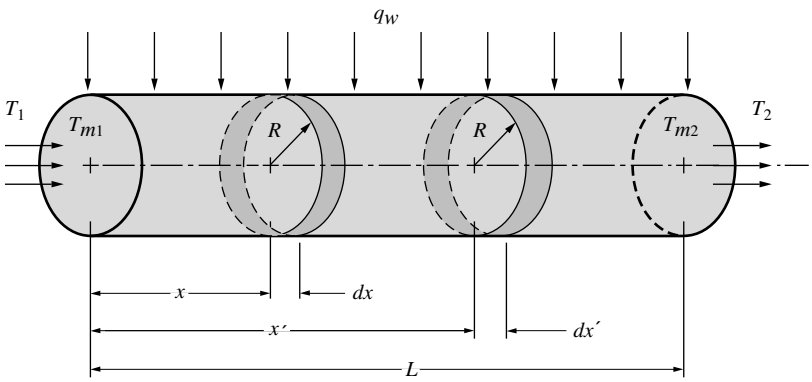

FIGURE 9-3
Forced convection and radiation of a transparent medium flowing through a circular tube, subject to constant wall heat flux.

or

$$\dot{m}\,c_p T_m(x) + h\,[T_w(x) - T_m(x)]\,2\pi R\,dx = \dot{m}\,c_p T_m(x+dx) = \dot{m}\,c_p \left[T_m(x) + \frac{dT_m}{dx}(x)\,dx\right], \tag{9.12}$$

or

$$\frac{dT_m}{dx} = \frac{2h}{\rho c_p u_m R}\,[T_w(x) - T_m(x)], \tag{9.13}$$

where axial conduction has been neglected, and the mass flow rate has been expressed in terms of mean velocity as $\dot{m} = \rho u_m \pi R^2$. Equation (9.13) is a single equation for the unknown wall and bulk temperatures $T_w(x)$ and $T_m(x)$ and is subject to the inlet condition

$$T_m(x=0) = T_{m1}. \tag{9.14}$$

An energy balance for the tube surface states that the prescribed heat flux q_w is dissipated by convection and radiation or, applying equation (5.26) for the radiative heat flux,

$$q_w = h\,[T_w(x) - T_m(x)] + \frac{\epsilon}{1-\epsilon}\left[\sigma T_w^4(x) - J(x)\right]. \tag{9.15}$$

The radiosity $J(x)$ is found from equation (5.24) as

$$J(x) = \epsilon\sigma T_w^4(x) + (1-\epsilon)\left\{\sigma T_1^4\,F_{dx-1} + \sigma T_2^4\,F_{dx-2} + \int_0^L J(x')\,dF_{dx-dx'}\right\}, \tag{9.16}$$

where F_{dx-1} is the view factor from the circular strip of width dx at x to the opening at $x=0$, F_{dx-2} is the one to the opening at $x=L$, and $dF_{dx-dx'}$ is the view factor between two circular strips located at x and x', as indicated in Fig. 9-3. All view factors are readily determined from Appendix D, Configurations 9 and 31, and will not be repeated here. Equations (9.13), (9.15), and (9.16) are a set of three simultaneous equations in the unknown $T_w(x)$, $T_m(x)$, and $J(x)$, which must be solved numerically. Before we attempt such a solution, it is best to recast the equations in nondimensional form. Defining the following variables and parameters,

$$\xi = \frac{x}{D}, \quad \theta(\xi) = \left(\frac{\sigma T^4}{q_w}\right)^{1/4}, \quad \mathscr{J}(\xi) = \frac{J}{q_w}, \tag{9.17a}$$

$$\mathrm{St} = \frac{h}{\rho c_p u_m}, \quad H = \frac{h}{q_w}\left(\frac{q_w}{\sigma}\right)^{1/4}, \tag{9.17b}$$

transforms equations (9.13) through (9.16) to

$$\frac{d\theta_m}{d\xi} = 4\,\mathrm{St}\,[\theta_w(\xi) - \theta_m(\xi)], \quad \theta_m(\xi=0) = \theta_{m1}, \tag{9.18}$$

$$1 = H\,[\theta_w(\xi) - \theta_m(\xi)] + \frac{\epsilon}{1-\epsilon}\left[\theta_w^4(\xi) - \mathscr{J}(\xi)\right], \tag{9.19}$$

$$\mathscr{J}(\xi) = \epsilon\,\theta_w^4(\xi) + (1-\epsilon)\left\{\theta_1^4 F_{d\xi-1} + \theta_2^4 F_{d\xi-2} + \int_0^{L/D} \mathscr{J}(\xi')\,dF_{d\xi-d\xi'}\right\}. \tag{9.20}$$

Equation (9.19) becomes indeterminate for $\epsilon = 1$. For the case of a black tube $\mathscr{J} = \theta_w^4$, and equations (9.19) and (9.20) may be combined as

$$1 = H\,[\theta_w(\xi) - \theta_m(\xi)] + \theta_w^4(\xi) - \theta_1^4 F_{d\xi-1} - \theta_2^4 F_{d\xi-2} - \int_0^{L/D} \theta_w^4(\xi')\,dF_{d\xi-d\xi'}. \tag{9.21}$$

Example 9.1. A transparent gas flows through a black tube subject to a constant heat flux. The convective heat transfer coefficient is known to be constant such that Stanton numbers and the nondimensional heat transfer coefficient are evaluated as $\mathrm{St} = 2.5 \times 10^{-3}$ and $H = 0.8$. The environmental temperatures at both ends are equal to the local gas temperatures, i.e., $\theta_1 = \theta_{m1}$ and $\theta_2 = \theta_{m2} = \theta_m(\xi = L/D)$, and the nondimensional inlet temperature is given as $\theta_{m1} = 1.5$. Determine the (nondimensional) wall temperature variation as a function of relative tube length, L/D, using the numerical quadrature approach of Example 5.11.

Solution

Since the tube wall is black we have only two simultaneous equations, (9.18) and (9.21), in the two unknowns θ_m and θ_w. However, the equations are nonlinear; therefore, an iterative procedure is necessary. For simplicity, we will adopt a simple backward finite-difference approach for the solution of equation (9.18), and the numerical quadrature scheme of equation (5.52) for the integral in equation (9.21). Evaluating temperatures at $N+1$ nodal points $\xi_i = i\Delta\xi$ ($i = 0, 1, \ldots, N$) where $\Delta\xi = L/(ND)$, this implies

$$\left(\frac{d\theta_m}{d\xi}\right)_{\xi_i} \simeq \frac{\theta_m(\xi_i) - \theta_m(\xi_{i-1})}{\Delta\xi}, \quad i = 1, 2, \ldots, N,$$

$$\int_0^{L/D} \theta_w^4(\xi') \frac{dF_{d\xi-d\xi'}}{d\xi'}\,d\xi' \simeq \frac{L}{D}\sum_{j=0}^{N} c_j\,\theta_w^4(\xi_j)\,K(\xi_i, \xi_j), \quad i = 0, 1, \ldots, N,$$

where the c_j are quadrature weights and, from Configuration 9 in Appendix D,[2]

$$K(\xi_i, \xi_j) = 1 - \frac{X_{ij}(2X_{ij}^2+3)}{2(X_{ij}^2+1)}; \quad X_{ij} = |\xi_i - \xi_j|.$$

Similarly, the two view factors to the openings are evaluated from Configuration 31 in Appendix D as

$$F_{d\xi_i-k} = \frac{X_{ij}^2 + \frac{1}{2}}{\sqrt{X_{ij}^2+1}} - X_{ij},$$

where

$$j = 0 \quad \text{if} \quad k = 1 \quad (\text{opening at } \xi = \xi_0 = 0),$$
$$j = N \quad \text{if} \quad k = 2 \quad (\text{opening at } \xi = \xi_N = L/D).$$

To solve for the unknown $\theta_m(\xi_i)$ and $\theta_w(\xi_i)$, we adopt the following iterative procedure:

1. A wall temperature is guessed for all wall nodes, say,

$$\theta_w(\xi_i) = \theta_1, \quad i = 0, 1, \ldots, N.$$

[2]Note that $K(\xi, \xi')$ has a sharp peak at $\xi' = \xi$. Therefore, and also in light of the truncation error in the finite-differencing of $d\theta_m/d\xi$, it is best to limit the quadrature scheme to Simpson's rule [43].

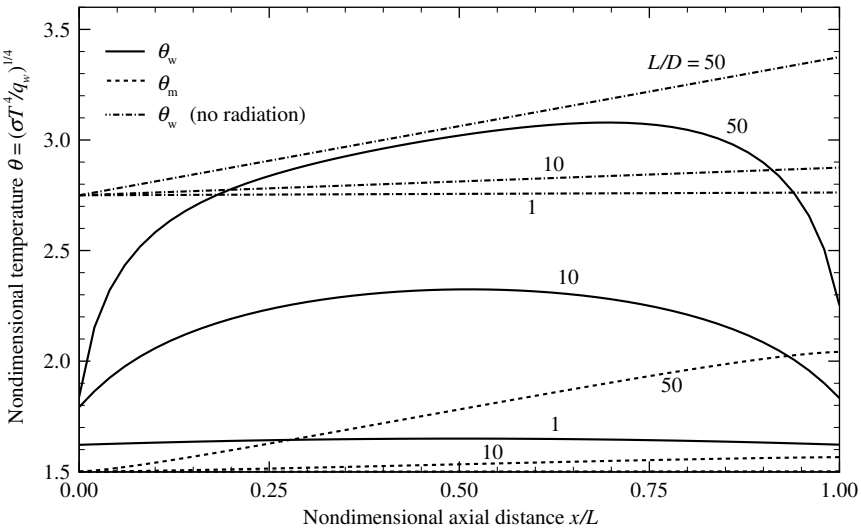

FIGURE 9-4
Axial surface temperature development for combined convection and surface radiation in a black tube subjected to constant wall heat flux.

2. A temperature difference is calculated from equation (9.21), i.e.,

$$\phi_i = H\,[\theta_w(\xi_i) - \theta_m(\xi_i)] = 1 - \theta_w^4(\xi_i) + \theta_1^4 F_{d\xi_i - 1} + \theta_2^4 F_{d\xi_i - 2} + \frac{L}{D}\sum_{j=0}^{N} c_j\,\theta_w^4(\xi_j)\,K(\xi_i, \xi_j).$$

3. The gas bulk temperature is calculated from equation (9.18) as

$$\theta_m(\xi_i) = \theta_m(\xi_{i-1}) + \frac{4\,\mathrm{St}\,\Delta\xi}{H}\phi_i; \quad \theta_m(\xi_0) = \theta_1.$$

4. An updated value for the wall temperatures is then determined from the definition for ϕ_i, that is,

$$\theta_w^{\mathrm{new}}(\xi_i) = \omega\left[\theta_m(\xi_i) + \frac{1}{H}\phi_i\right] + (1-\omega)\,\theta_w^{\mathrm{old}}(\xi_i),$$

where ω is known as the *relaxation parameter*. The iteration scheme is called underrelaxed if $\omega < 1$, and overrelaxed if $\omega > 1$. If ω is chosen too large, the iteration will become unstable and not converge at all. A good or optimal value for the relaxation parameter must usually be found by trial and error. Detailed discussions on relaxation may be found in standard numerical analysis texts such as [44,45]. Some representative results are shown in Fig. 9-4 for several values of L/D. Because of the strong nonlinearity of the problem, and the crude numerical scheme employed here, large numbers of nodes are necessary to achieve good accuracy ($N \simeq 40L/D$), together with strong underrelaxation ($\omega < 0.02$).

For the case of pure convection ($\epsilon = 0$, or $\phi_i \equiv 1$) the tube wall temperature rises linearly with axial distance, since constant wall heat flux implies a linear increase in bulk temperature and, therefore, (assuming a constant heat transfer coefficient) in surface temperature. This is not the case if radiation is present, in particular for short tubes (small L/D). Near both ends of the tube, much of the radiative energy leaves through the openings, causing a distinct drop in surface temperature. For long tubes ($L/D > 50$) the surface temperature rises almost linearly over the central parts of the tube, although the temperature stays below the convection-only case: Due to the higher temperatures downstream, some net radiative heat flux travels upstream, making overall heat transfer a little more efficient. It should be noted here that the assumption of a constant heat transfer coefficient is not particularly realistic, since it implies a fully developed thermal profile. It is well known that for pure convection $h \to \infty$ at the inlet and, thus, $\theta_w(\xi = 0) = 1$ [1]. Near the inlet of a tube the actual temperature distribution for pure convection is very similar to the one depicted in Fig. 9-3, which is driven by radiation losses. Although for pure convection a fully developed thermal profile and constant h are eventually reached

(at $L/D > 20$ for turbulent flow), in the presence of radiation a constant heat transfer coefficient is *never* reached (because the radiation term makes the governing equations nonlinear).

A number of researchers have investigated combined convection and radiation for a transparent flowing medium. Flow through circular tubes was considered by Siegel and coworkers [46–48] for a number of situations, but always assuming a constant and known heat transfer coefficient. Dussan and Irvine [49] and Chen [50] calculated the local convection rate by solving the two-dimensional energy equation for the flowing medium, but they made severe simplifications in the evaluation of radiative heat fluxes. The most general tube flow analysis has been carried out by Thorsen and Kanchanagom [51, 52]. Similar problems for parallel-plate channel flow were investigated by Keshock and Siegel [53] (for a constant heat transfer coefficient) and Lin and Thorsen [54] (for two-dimensional convection calculations). Combined radiation and forced convection of external flow across a flat plate has been addressed by Cess [55,56], Sparrow and Lin [57], and Sohal and Howell [58]. Fluidized bed heat transfer has also been investigated by a number of researchers [59–61] and, finally, the interaction between surface radiation and free convection has been studied, both numerically and experimentally [62–71].

References

1. Holman, J. P.: *Heat Transfer*, 7th ed., McGraw-Hill Book Company, New York, 1990.
2. Sparrow, E. M., E. R. G. Eckert, and T. F. Irvine: "The effectiveness of radiating fins with mutual irradiation," *Journal of the Aerospace Sciences*, no. 28, pp. 763–772, 1961.
3. Hering, R. G.: "Radiative heat exchange between conducting plates with specular reflection," *ASME Journal of Heat Transfer*, vol. C88, pp. 29–36, 1966.
4. Tien, C. L.: "Approximate solutions of radiative exchange between conducting plates with specular reflection," *ASME Journal of Heat Transfer*, vol. 89C, pp. 119–120, 1967.
5. Bartas, J. G., and W. H. Sellers: "Radiation fin effectiveness," *ASME Journal of Heat Transfer*, vol. 82C, pp. 73–75, 1960.
6. Sparrow, E. M., and E. R. G. Eckert: "Radiant interaction between fins and base surfaces," *ASME Journal of Heat Transfer*, vol. C84, pp. 12–18, 1962.
7. Sparrow, E. M., V. K. Jonsson, and W. J. Minkowycz: "Heat transfer from fin-tube radiators including longitudinal heat conduction and radiant interchange between longitudinally non-isothermal finite surfaces," *NASA TN D-2077*, 1963.
8. Lieblein, S.: "Analysis of temperature distribution and radiant heat transfer along a rectangular fin," *NASA TN D-196*, 1959.
9. Chambers, R. L., and E. V. Sommers: "Radiation fin efficiency for one-dimensional heat flow in a circular fin," *ASME Journal of Heat Transfer*, vol. 81C, no. 4, pp. 327–329, 1959.
10. Keller, H. H., and E. S. Holdredge: "Radiation heat transfer for annular fins of trapezoid profile," *ASME Journal of Heat Transfer*, vol. 92, no. 6, pp. 113–116, 1970.
11. Mackay, D. B.: *Design of Space Powerplants*, Prentice-Hall, Englewood Cliffs, NJ, 1963.
12. Sparrow, E. M., G. B. Miller, and V. K. Jonsson: "Radiating effectiveness of annular-finned space radiators including mutual irradiation between radiator elements," *Journal of Aerospace Sciences*, vol. 29, pp. 1291–1299, 1962.
13. Abarbanel, S. S.: "Time dependent temperature distribution in radiating solids," *J. Math. Phys.*, vol. 39, no. 4, pp. 246–257, 1960.
14. Eckert, E. R. G., T. F. Irvine, and E. M. Sparrow: "Analytical formulation for radiating fins with mutual irradiation," *American Rocket Society Journal*, vol. 30, pp. 644–646, 1960.
15. Nilson, E. N., and R. Curry: "The minimum weight straight fin of triangular profile radiating to space," *Journal of the Aerospace Sciences*, vol. 27, p. 146, 1960.
16. Hickman, R. S.: "Transient response and steady-state temperature distribution in a heated, radiating, circular plate," Technical Report 32-169, California Institute of Technology, Jet Propulsion Laboratory, 1961.
17. Heaslet, M. A., and H. Lomax: "Numerical predictions of radiative interchange between conducting fins with mutual irradiations," *NASA TR R-116*, 1961.
18. Nichols, L. D.: "Surface-temperature distribution on thin-walled bodies subjected to solar radiation in interplanetary space," *NASA TN D-584*, 1961.
19. Schreiber, L. H., R. P. Mitchell, G. D. Gillespie, and T. M. Olcott: "Techniques for optimization of a finned-tube radiator," *ASME Paper No. 61-SA-44*, June 1961.
20. Olmstead, W. E., and S. Raynor: "Solar heating of a rotating spherical space vehicle," *International Journal of Heat and Mass Transfer*, vol. 5, pp. 1165–1177, 1962.
21. Wilkins, J. E.: "Minimum-mass thin fins and constant temperature gradients," *J. Soc. Ind. Appl. Math*, vol. 10, no. 1, pp. 62–73, 1962.

22. Hrycak, P.: "Influence of conduction on spacecraft skin temperatures," *AIAA Journal*, vol. 1, pp. 2619–2621, 1963.
23. Karlekar, B. V., and B. T. Chao: "Mass minimization of radiating trapezoidal fins with negligible base cylinder interaction," *International Journal of Heat and Mass Transfer*, vol. 6, pp. 33–48, 1963.
24. Stockman, N. O., and J. L. Kramer: "Effect of variable thermal properties on one-dimensional heat transfer in radiating fins," *NASA TN D-1878*, 1963.
25. Kotan, K., and O. A. Arnas: "On the optimization of the design parameters of parabolic radiating fins," *ASME Paper No. 65-HT-42*, August 1965.
26. Mueller, H. F., and N. D. Malmuth: "Temperature distribution in radiating heat shields by the method of singular perturbations," *International Journal of Heat and Mass Transfer*, vol. 8, pp. 915–920, 1965.
27. Russell, L. D., and A. J. Chapman: "Analytical solution of the 'known-heat-load' space radiator problem," *Journal of Spacecraft and Rockets*, vol. 4, no. 3, pp. 311–315, 1967.
28. Frost, W., and A. H. Eraslan: "An iterative method for determining the heat transfer from a fin with radiative interaction between the base and adjacent fin surfaces," *AIAA Paper No. 68-772*, June 1968.
29. Donovan, R. C., and W. M. Rohrer: "Radiative conducting fins on a plane wall, including mutual irradiation," *ASME Paper No. 69-WA/HT-22*, November 1969.
30. Schnurr, N. M., A. B. Shapiro, and M. A. Townsend: "Optimization of radiating fin arrays with respect to weight," *ASME Journal of Heat Transfer*, vol. 98, no. 4, pp. 643–648, 1976.
31. Eslinger, R., and B. Chung: "Periodic heat transfer in radiating and convecting fins or fin arrays," *AIAA Journal*, vol. 17, no. 10, pp. 1134–1140, 1979.
32. Gerencser, D. S., and A. Razani: "Optimization of radiative–convective arrays of pins fins including mutual irradiation between fins," *International Journal of Heat and Mass Transfer*, vol. 38, pp. 899–907, 1995.
33. Chung, B. T. F., B. X. Zhang, and E. T. Lee: "A multi-objective optimization of radiative fin array systems in a fuzzy environment," *ASME Journal of Heat Transfer*, vol. 118, no. 3, pp. 642–649, 1996.
34. Krishnaprakas, C. K.: "Optimum design of radiating rectangular plate fin array extending from a plane wall," *ASME Journal of Heat Transfer*, vol. 118, pp. 490–493, 1996.
35. Krishnaprakas, C. K.: "Optimum design of radiating longitudinal fin array extending from a cylindrical surface," *ASME Journal of Heat Transfer*, vol. 119, pp. 857–860, 1997.
36. Fitzgerald, S. P., and W. Strieder: "Radiation heat transfer down an elongated spheroidal cavity," *AIChE Journal*, vol. 43, pp. 2–12, 1997.
37. Liang, X. G., and W. Qu: "Effective thermal conductivity of gas–solid composite materials and the temperature difference effect at high temperature," *International Journal of Heat and Mass Transfer*, vol. 42, no. 10, pp. 1885–1893, 1999.
38. Singh, B. P., and M. Kaviany: "Effect of solid conductivity on radiative heat transfer in packed beds," *International Journal of Heat and Mass Transfer*, vol. 37, no. 16, pp. 2579–2583, 1994.
39. Haya, R., D. Rivas, and J. Sanz: "Radiative exchange between a cylindrical crystal and a monoellipsoidal mirror furnace," *International Journal of Heat and Mass Transfer*, vol. 40, pp. 323–332, 1997.
40. Hollands, K. G. T., and K. Iynkaran: "Analytical model for the thermal conductance of compound honeycomb transparent insulation, with experimental validation," *Solar Energy*, vol. 51, pp. 223–227, 1993.
41. Jones, P. D.: "Correlation of combined radiation and conduction in evacuated honeycomb-cored panels," *Journal of Solar Energy Engineering*, vol. 118, pp. 97–100, 1996.
42. Schweiger, H., A. Oliva, M. Costa, and C. D. Segarra: "Monte Carlo method for the simulation of transient radiation heat transfer: Application to compound honeycomb transparent insulation," *Numerical Heat Transfer – Part B: Fundamentals*, vol. 35, pp. 113–136, 1999.
43. Fröberg, C. E.: *Introduction to Numerical Analysis*, Addison-Wesley, Reading, MA, 1969.
44. Hornbeck, R. W.: *Numerical Methods*, Quantum Publishers, Inc., New York, 1975.
45. Ferziger, J. H.: *Numerical Methods for Engineering Application*, John Wiley & Sons, New York, 1981.
46. Siegel, R., and M. Perlmutter: "Convective and radiant heat transfer for flow of a transparent gas in a tube with gray wall," *International Journal of Heat and Mass Transfer*, vol. 5, pp. 639–660, 1962.
47. Perlmutter, M., and R. Siegel: "Heat transfer by combined forced convection and thermal radiation in a heated tube," *ASME Journal of Heat Transfer*, vol. C84, pp. 301–311, 1962.
48. Siegel, R., and E. G. Keshock: "Wall temperature in a tube with forced convection, internal radiation exchange and axial wall conduction," *NASA TN D-2116*, 1964.
49. Dussan, B. I., and T. F. Irvine: "Laminar heat transfer in a round tube with radiating flux at the outer wall," in *Proceedings of the Third International Heat Transfer Conference*, vol. 5, Hemisphere, Washington, D.C., pp. 184–189, 1966.
50. Chen, J. C.: "Laminar heat transfer in a tube with nonlinear radiant heat-flux boundary conditions," *International Journal of Heat and Mass Transfer*, vol. 9, pp. 433–440, 1966.
51. Thorsen, R. S.: "Heat transfer in a tube with forced convection, internal radiation exchange, axial wall heat conduction and arbitrary wall heat generation," *International Journal of Heat and Mass Transfer*, vol. 12, pp. 1182–1187, 1969.
52. Thorsen, R. S., and D. Kanchanagom: "The influence of internal radiation exchange, arbitrary wall heat generation and wall heat conduction on heat transfer in laminar and turbulent flows," in *Proceedings of the Fourth International Heat Transfer Conference*, vol. 3, Elsevier, New York, pp. 1–10, 1970.
53. Keshock, E. G., and R. Siegel: "Combined radiation and convection in asymmetrically heated parallel plate flow channel," *ASME Journal of Heat Transfer*, vol. 86C, pp. 341–350, 1964.

54. Lin, S. T., and R. S. Thorsen: "Combined forced convection and radiation heat transfer in asymmetrically heated parallel plates," in *Proceedings of the Heat Transfer and Fluid Mechanics Institute*, Stanford University Press, pp. 32–44, 1970.
55. Cess, R. D.: "The effect of radiation upon forced-convection heat transfer," *Applied Scientific Research Part A*, vol. 10, pp. 430–438, 1962.
56. Cess, R. D.: "The interaction of thermal radiation with conduction and convection heat transfer," in *Advances in Heat Transfer*, vol. 1, Academic Press, New York, pp. 1–50, 1964.
57. Sparrow, E. M., and S. H. Lin: "Boundary layers with prescribed heat flux–application to simultaneous convection and radiation," *International Journal of Heat and Mass Transfer*, vol. 8, pp. 437–448, 1965.
58. Sohal, M., and J. R. Howell: "Determination of plate temperature in case of combined conduction, convection and radiation heat exchange," *International Journal of Heat and Mass Transfer*, vol. 16, pp. 2055–2066, 1973.
59. Flamant, G., J. D. Lu, and B. Variot: "Radiation heat transfer in fluidized beds: A comparison of exact and simplified approaches," *ASME Journal of Heat Transfer*, vol. 116, no. 3, pp. 652–659, 1994.
60. Fang, Z. H., J. R. Grace, and C. J. Lim: "Radiative heat transfer in circulating fluidized beds," *ASME Journal of Heat Transfer*, vol. 117, no. 4, pp. 963–968, 1995.
61. Luan, W., C. J. Lim, C. M. H. Brereton, B. D. Bowen, and J. R. Grace: "Experimental and theoretical study of total and radiative heat transfer in circulating fluidized beds," *Chemical Engineering and Science*, vol. 54, no. 17, pp. 3749–3764, 1999.
62. Gianoulakis, S., and D. E. Klein: "Combined natural convection and surface radiation in the annular region between volumetrically heated inner tube and a finite conducting outer tube," *Nuclear Technology*, vol. 104, pp. 241–251, 1993.
63. Balaji, C., and S. P. Venkateshan: "Natural convection in L-corners with surface radiation and conduction," *ASME Journal of Heat Transfer*, vol. 118, pp. 222–225, 1996.
64. Rao, V. R., and S. P. Venkateshan: "Experimental study of free convection and radiation in horizontal fin arrays," *International Journal of Heat and Mass Transfer*, vol. 39, pp. 779–789, 1996.
65. Rao, V. R., C. Balaji, and S. P. Venkateshan: "Interferometric study of interaction of free convection with surface radiation in an l corner," *International Journal of Heat and Mass Transfer*, vol. 40, pp. 2941–2947, 1997.
66. Jayaram, K. S., C. Balaji, and S. P. Venkateshan: "Interaction of surface radiation and free convection in an enclosure with a vertical partition," *ASME Journal of Heat Transfer*, vol. 119, pp. 641–645, 1997.
67. Cheng, X., and U. Müller: "Turbulent natural convection coupled with thermal radiation in large vertical channels with asymmetric heating," *International Journal of Heat and Mass Transfer*, vol. 41, no. 12, pp. 1681–1692, 1998.
68. Ramesh, N., and S. P. Venkateshan: "Effect of surface radiation on natural convection in a square enclosure," *Journal of Thermophysics and Heat Transfer*, vol. 13, no. 3, pp. 299–301, 1999.
69. Yu, E., and Y. K. Joshi: "Heat transfer in discretely heated side-vented compact enclosures by combined conduction, natural convection, and radiation," *ASME Journal of Heat Transfer*, vol. 121, no. 4, pp. 1002–1010, 1999.
70. Adams, V. H., Y. K. Joshi, and D. L. Blackburn: "Three-dimensional study of combined conduction, radiation, and natural convection from discrete heat sources in a horizontal narrow-aspect-ratio enclosure," *ASME Journal of Heat Transfer*, vol. 121, no. 4, pp. 992–1001, 1999.
71. Velusamy, K., T. Sundararajan, and K. N. Seetharamu: "Interaction effects between surface radiation and turbulent natural convection in square and rectangular enclosures," *ASME Journal of Heat Transfer*, vol. 123, no. 6, pp. 1062–1070, 2001.
72. Vader, D. T., R. Viskanta, and F. P. Incropera: "Design and testing of a high-temperature emissometer for porous and particulate dielectrics," *Review of Scientific Instruments*, vol. 57, no. 1, pp. 87–93, 1986.
73. Sikka, K. K.: "High temperature normal spectral emittance of silicon carbide based materials," M.S. thesis, The Pennsylvania State University, University Park, PA, 1991.

Problems

9.1 A satellite shaped like a sphere ($R = 1\,\text{m}$) has a gray-diffuse surface coating with $\epsilon_s = 0.3$ and is fitted with a long, thin, cylindrical antenna, as shown in the adjacent sketch. The antenna is a specular reflector with $\epsilon_a = 0.1$, $k_a = 100\,\text{W/m K}$, and $d = 1\,\text{cm}$. Satellite and antenna are exposed to solar radiation of strength $q_{\text{sol}} = 1300\,\text{W/m}^2$ from a direction normal to the antenna. Assuming that the satellite produces heat at a rate of 4 kW and—due to a high-conductivity shell—is essentially isothermal, determine the equilibrium temperature distribution along the antenna. (Hint: Use the fact that $d \ll R$ not only for conduction calculations, but also for the calculation of view factors.)

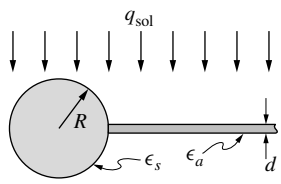

9.2 A long, thin, cylindrical needle ($L \gg D$) is attached perpendicularly to a large, isothermal base plate at $T = T_b = \text{const}$. The base plate is gray and diffuse ($\epsilon_b = \alpha_b$), while the needle is nongray and diffuse ($\epsilon \neq \alpha$). The needle exchanges heat by convection and radiation with a large, isothermal environment at T_∞.

(*a*) Neglecting heat losses from the free tip of the needle, formulate the problem for the calculation of needle temperature distribution, total heat loss, and fin efficiency.

(*b*) Implement the solution numerically for $L = 1\,\text{m}$, $D = 1\,\text{cm}$, $k = 10\,\text{W/m K}$, $h = 40\,\text{W/m}^2\,\text{K}$, $\epsilon = 0.8$, $\alpha = 0.4$, $\epsilon_b = 0.8$, $T_b = 1000\,\text{K}$, $T_\infty = 300\,\text{K}$.

9.3 In the emissometer of Vader and coworkers [72] and Sikka [73], the sample is kept inside a long silicon carbide tube that in turn, is inside a furnace, as shown in the sketch. The furnace is heated with a number of SiC heating elements, providing a uniform flux over a 45 cm length as shown. Assume that there is no heat loss through the refractory brick or the bottom of the furnace, that the inside heat transfer coefficient for free convection (with air at 600°C) is $10\,\text{W/m}^2\,\text{K}$, that the silicon carbide tube is gray-diffuse ($\epsilon = 0.9$, $k = 100\,\text{W/m K}$), and that the sample temperature is equal to the SiC tube temperature at the same height. What must be the steady-state power load on the furnace to maintain a sample temperature of 1000°C? In this configuration a detector receiving radiation from a small center spot of the sample is supposedly getting the same amount as from a blackbody at 1000°C (cf. Table 5.1). What is the actual emittance sensed by the detector, i.e., what systematic error is caused by this near-blackbody, if the sample is gray and diffuse with $\epsilon_s = 0.5$?

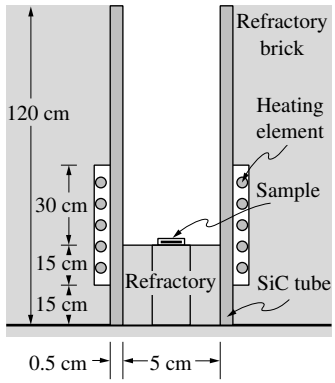

9.4 A thermocouple with a 0.5 mm diameter bead is used to measure the local temperature of a hot, radiatively nonparticipating gas flowing through an isothermal, gray-diffuse tube ($T_w = 300\,\text{K}$, $\epsilon_w = 0.8$). The thermocouple is a diffuse emitter/specular reflector with $\epsilon_b = 0.5$, and the heat transfer coefficient between bead and gas is $30\,\text{W/m}^2\,\text{K}$.

(*a*) Determine the thermocouple error as a function of gas temperature (i.e., $|T_b - T_g|$ *vs.* T_g).

(*b*) In order to reduce the error, a radiation shield in the form of a thin, stainless-steel cylinder ($\epsilon = 0.1$, $R = 2\,\text{mm}$, $L = 20\,\text{mm}$) is placed over the thermocouple. This also reduces the heat transfer coefficient between bead and gas to $15\,\text{W/m}^2\,\text{K}$, which is equal to the heat transfer coefficient on the inside of the shield. On the outside of the cylinder the heat transfer coefficient is $30\,\text{W/m}^2\,\text{K}$. Determine error *vs.* gas temperature for this case.

To simplify the problem, you may make the following assumptions: (*i*) the leads of the thermocouple may be neglected, (*ii*) the shield is very long as far as the radiation analysis is concerned, and (*iii*) the shield reflects diffusely.

9.5 Repeat Problem 5.36 for the case in which a radiatively nonparticipating, stationary gas ($k = 0.04$ W/m K) is filling the 1 cm thick gap between surface and shield.